Signal Processing 140 (2017) 110–115

Contents lists available at ScienceDirect

Signal Processing

journal homepage: www.elsevier.com/locate/sigpro

A weighted detector for mismatched subspace signals

Jun Liu[a,b], Kai Li[c], Xichuan Zhang[d], Ming Liu[d], Weijian Liu[d,*]

[a] National Laboratory of Radar Signal Processing, Xidian University, Xi'an, 710071, China
[b] Collaborative Innovation Center of Information Sensing and Understanding, Xidian University, Xi'an, 710071, China
[c] School of Electronic Information, Wuhan University, Wuhan 430072, China
[d] Wuhan Electronic Information Institute, Wuhan 430019, China

ARTICLE INFO

Article history:
Received 20 January 2017
Revised 5 May 2017
Accepted 8 May 2017
Available online 16 May 2017

Keywords:
Adaptive detection
Multichannel signal detection
Subspace signal mismatch
Statistical distribution

ABSTRACT

This paper investigates the problem of detecting a multichannel signal when subspace signal mismatch occurs. A new detector is proposed, which is obtained by weighting two existing detectors, namely, the subspace-based adaptive matched filter and adaptive subspace detector. The proposed weighted detector has flexibility in controlling its capability of rejection mismatched subspace signals. Specifically, its robustness (or selectivity) for mismatched subspace signals improves as the weight value increases (or decreases). Closed-form expressions for the probabilities of detection and false alarm are derived. The theoretical results are confirmed by Monte Carlo simulations.

1. Introduction

Detection of a signal embedded in noise is a common problem in the field of signal processing. Kelly was the first adopting the generalized likelihood ratio test (GLRT) to multichannel signal detection [1]. Then Chen et al. [2] and Robey et al. [3] independently derive the adaptive matched filter (AMF), which has lower complexity than the KGLRT. For the same detection problem in [1], De Maio derives the Rao test, denoted as De Maio's Rao (DMRao) [4]. The DMRao provides better performance than the KGLRT and AMF in rejecting mismatched signals. Note that these three detectors are designed in homogeneous environment, where the test and training data have the same noise covariance matrix. In [5], the detection problem in partially homogeneous environment is exploited and the adaptive coherence estimate (ACE) is proposed therein. For partially homogeneous environment, the test and training data share the same covariance matrix up to an unknown scaling factor. Recently, many different kinds of detection problems are investigated and a large number of detectors are proposed, such as [6–16] and the references therein.

The detectors mentioned above are mainly devised in the absence of signal mismatch. However, signal mismatch often happens due to array errors, pointing errors, and wavefront distortions [17]. It is worth noting that robust detectors are not always preferred [17]. For example, when a target is located in the sidelobe of the radar beam, there is mismatch between the target bearing and radar beam steering. Hence, it is often desirable to reject this sidelobe target (for the purpose of target localization) and wait until it enters into the main beam. As a result, in some practical applications one needs a detector which can balance the robustness and selectivity [18]. The capability of a detector to reject or detect mismatched signals is referred to as the directivity [19]. In the open literature there are mainly two kinds of methods to make tradeoff between robustness and selectivity. One is the two-stage detection scheme. A two-stage detector is constructed by cascading two detectors, which usually behave quite differently in the case of signal mismatch. Precisely, one detector is selective[1] to signal mismatch, while the other is robust to signal mismatch. The two-stage detector have two detection thresholds. By tuning the pair of detection thresholds for a fixed probability of false alarm (PFA), the two-stage detector achieves flexible robustness to mismatched signals. The well-known two-stage detectors are the adaptive sidelobe blanker (ASB) [20], the two-stage detector cascading the AMF and KGLRT [21], the two-stage Rao test cascading of the AMF and DMRao [4], the so-called WAS-ASB cascading the subspace-based GLRT (SGLRT) and whited-adaptive beamforming orthogonal rejection test (W-ABORT) [22], the subspace-based ASB (S-ASB) cascading the SGLRT and ACE [23], the so-called KWAS-ASB cascading the SGLRT and KWA [24], and the two-stage Rao test cascading the SGLRT and DMRao [25]. More recently, a review of two-stage detectors is given in [19]. The other kind of method to solve the de-

* Corresponding author.
E-mail address: liuvjian@163.com (W. Liu).

[1] A selective detector is less tolerant to signal mismatch. When signal mismatch occurs, the probability of detection (PD) of a selective rapidly decreases.

http://dx.doi.org/10.1016/j.sigpro.2017.05.011
0165-1684/

tection problem in the presence of signal mismatch is the tunable detector (or called the parametric detector). The tunable detector is parameterized by a scalar, referred to as the tunable parameter. By changing the tunable parameter, the tunable detector can smoothly varying from a robust detector to a selective one. Many tunable detectors have been proposed, such as the tunable detector given in [26], the KWA [24], the KRAO [27], and the KMABORT [28].

Note that all the two-stage detectors and tunable detectors mentioned above are designed for rank-one signals, which have known signal steering vectors. However, in many applications the actual signal may be naturally a subspace signal, such as the polarimetric signal [29], which belongs to a known subspace but with unknown coordinates. Signal mismatch can also arise for subspace signals, due to the same reasons for rank-one signals. Subspace signal mismatch is defined as the phenomenon that the actual signal does not fully lie in the presumed subspace. Very limited works are done for subspace signal mismatch. In particular, several robust detectors are devised in [30–32] for subspace signal mismatch. However, a robust detector is not always a desirable choice.

In this paper, a kind of approach to signal detection in the presence of mismatched subspace signals is introduced. A new detector is constructed by weighting the subspace-based AMF (SAMF) [33] and adaptive subspace detector (ASD) [34]. For convenience, the proposed weighted detector is referred to as the SAMF-ASD. Note that the SAMF and ASD behave quite differently when subspace signal mismatch happens. Precisely, the SAMF is very robust, while the ASD is quite selective. As a consequence, the proposed SAMF-ASD is of great flexibility in controlling the detection performance for mismatched subspace signals. By adjusting the weight, the proposed SAMF-ASD can smoothly vary from a robust detector to a selective one. Analytical expressions for the PD and PFA are derived, which are verified by Monte Carlo (MC) simulations.

The rest of the paper is organized as follows. Section 2 gives the problem formulation and presents the proposed weighted detector. Section 3 shows the derivations of the analytical expressions for the PD and PFA in the case of subspace signal mismatch. Numerical examples are given in Section 4. Finally, Section 5 summarizes the paper.

2. Problem formulation and the proposed weighted detector

For a binary hypothesis test, one needs to make a decision between signal-presence and signal-absence choices. Denote the test data by an $N \times 1$ vector $\mathbf{x}$. Under the signal-absence hypothesis H_0, $\mathbf{x}$ can be expressed as $\mathbf{x} = \mathbf{n}$, where $\mathbf{n}$ is the noise, subjected to a zero-mean complex circular Gaussian distribution, with an unknown positive definite covariance matrix[2] $\mathbf{R}_t$. Under the signal-presence hypothesis H_1, $\mathbf{x} = \mathbf{s} + \mathbf{n}$, where $\mathbf{s}$ is the signal component with the form $\mathbf{s} = \mathbf{H}\boldsymbol{\theta}$. The $N \times p$ signal matrix $\mathbf{H}$ is known full-column-rank, whose columns span the nominal subspace where the signal is assumed to lie, and the $p \times 1$ vector $\boldsymbol{\theta}$ is deterministic but unknown, standing for the corresponding coordinate. In summary, the detection problem can be written symbolically as

$$\begin{cases} H_0 : \mathbf{x} = \mathbf{n}, \\ H_1 : \mathbf{x} = \mathbf{H}\boldsymbol{\theta} + \mathbf{n}. \end{cases} \tag{1}$$

Note that the noise covariance matrix $\mathbf{R}_t$ is unknown in practice. In order to estimate $\mathbf{R}_t$, a set of independent and identically distributed (IID) training data is needed, denoted by $\mathbf{x}_l$, $l = 1, 2, \cdots, L$. The training data $\mathbf{x}_l$ does not contain any signal but noise $\mathbf{n}_l$, which is subject to a zero-mean complex circular Gaussian distribution with a covariance matrix $\mathbf{R}$.

In homogeneous environment the noise in the test data and training data has the identical covariance matrix, i.e., $\mathbf{R}_t = \mathbf{R}$, while in partially homogeneous environment $\mathbf{R}_t = \sigma^2\mathbf{R}$. The scaling factor σ^2 is unknown, and it stands for the power mismatch between the test and training data. In homogeneous environment, according to the detector design criterion of two-step GLRT [33] or Wald test [35], one can obtain the SAMF

$$t_{\mathrm{SAMF}} = \mathbf{x}^H\mathbf{S}^{-1}\mathbf{H}(\mathbf{H}^H\mathbf{S}^{-1}\mathbf{H})^{-1}\mathbf{H}^H\mathbf{S}^{-1}\mathbf{x} \underset{H_0}{\overset{H_1}{\gtrless}} \eta_{\mathrm{m}}, \tag{2}$$

where $\mathbf{S} = \sum_{l=1}^{L}\mathbf{x}_l\mathbf{x}_l^H$ is L times the sample covariance matrix (SCM) and η_{m} is the detection threshold for the SAMF.

In the partially homogeneous environment, the GLRT for the detection problem in (1) is the ASD [34]

$$t'_{\mathrm{ASD}} = \frac{\mathbf{x}^H\mathbf{S}^{-1}\mathbf{H}(\mathbf{H}^H\mathbf{S}^{-1}\mathbf{H})^{-1}\mathbf{H}^H\mathbf{S}^{-1}\mathbf{x}}{\mathbf{x}^H\mathbf{S}^{-1}\mathbf{x}} \underset{H_0}{\overset{H_1}{\gtrless}} \eta'_{\mathrm{s}}, \tag{3}$$

where η'_{s} is the detection threshold for the ASD. Note that (3) is equivalent to

$$t_{\mathrm{ASD}} = \frac{\mathbf{x}^H\mathbf{S}^{-1}\mathbf{H}(\mathbf{H}^H\mathbf{S}^{-1}\mathbf{H})^{-1}\mathbf{H}^H\mathbf{S}^{-1}\mathbf{x}}{\mathbf{x}^H\mathbf{S}^{-1}\mathbf{x} - \mathbf{x}^H\mathbf{S}^{-1}\mathbf{H}(\mathbf{H}^H\mathbf{S}^{-1}\mathbf{H})^{-1}\mathbf{H}^H\mathbf{S}^{-1}\mathbf{x}} \underset{H_0}{\overset{H_1}{\gtrless}} \eta_{\mathrm{s}}, \tag{4}$$

since $t_{\mathrm{ASD}} = [(t'_{\mathrm{ASD}})^{-1} - 1]^{-1}$ is a monotonically increasing function of t'_{ASD}. In (4) η_{s} is the modified detection threshold given by $\eta_{\mathrm{s}} = [(\eta'_{\mathrm{s}})^{-1} - 1]^{-1}$.

Remarkably, the SAMF is very robust to subspace signal mismatch, while the ASD is very selective [36]. Unfortunately, the robustness of the SAMF or the selectivity of the ASD cannot be flexibly adjusted. Hence, a new detector is designed in this paper by weighting the SAMF and ASD, i.e.,

$$t_{\mathrm{SAMF-ASD}} = \alpha t_{\mathrm{SAMF}} + (1-\alpha)t_{\mathrm{ASD}} \underset{H_0}{\overset{H_1}{\gtrless}} \eta_{\mathrm{w}}, \tag{5}$$

where η_{w} is the detection threshold. For convenience, the proposed detector is referred to as the SAMF-ASD. A prominent property of the SAMF-ASD lies in flexibly adjusting its rejection capability for mismatched subspace signals. In (5) α is the weighted value, constrained to satisfy

$$0 \le \alpha \le 1. \tag{6}$$

Obviously, the SAMF-ASD with $\alpha = 0$ reduces to the ASD, while the SAMF-ASD with $\alpha = 1$ degenerates into the SAMF. An immediate remark on the proposed weighted detector is that it possesses the CFAR property with respect to the noise covariance matrix $\mathbf{R}$, since the SAMF and ASD are both CFAR[3] [33,34]. Moreover, the proposed SAMF-ASD is invariant with respect to the group of transformations defined in [37].

3. Statistical performance of the SAMF-ASD

This section exploits the statistical performance of the SAMF-ASD in the presence of subspace signal mismatch, for which the actual signal, say $\mathbf{s}_0$, does not completely lie in the subspace spanned by the nominal signal matrix $\mathbf{H}$. The PD of the SAMF-ASD can be expressed as

$$\mathrm{PD} = \Pr[t_{\mathrm{SAMF-ASD}} > \eta_{\mathrm{w}}; H_1], \tag{7}$$

where $\Pr[\,\cdot\,]$ stands for the probability of the event in the bracket and η_{w} is the detection threshold for the SAMF-ASD.

[2] Note that the covariance matrix is equal to the correlation matrix, since the mean of the noise is zero. This reasoning is also valid for the SCM given in (2).

[3] Note that ASD has additional CFAR property with respect to the power mismatch between the training and the test data. However, in this paper, it mainly focuses on the case of homogeneous environment.

To obtain the expressions for the PD and PFA of the SAMF-ASD, the statistical dependence of the SAMF and ASD on the SGLRT and a loss factor is used. The statistical distributions of the SGLRT and the loss factor in the case of subspace signal mismatch are given in [36]. The detection statistic of the SGLRT is [38]

$$t_{\mathrm{SGLRT}} = \frac{\mathbf{x}^H\mathbf{S}^{-1}\mathbf{H}(\mathbf{H}^H\mathbf{S}^{-1}\mathbf{H})^{-1}\mathbf{H}^H\mathbf{S}^{-1}\mathbf{x}}{1+\mathbf{x}^H\mathbf{S}^{-1}\mathbf{x}-\mathbf{x}^H\mathbf{S}^{-1}\mathbf{H}(\mathbf{H}^H\mathbf{S}^{-1}\mathbf{H})^{-1}\mathbf{H}^H\mathbf{S}^{-1}\mathbf{x}}, \tag{8}$$

while the loss factor is defined as

$$\beta = \frac{1}{1+\mathbf{x}^H\mathbf{S}^{-1}\mathbf{x}-\mathbf{x}^H\mathbf{S}^{-1}\mathbf{H}(\mathbf{H}^H\mathbf{S}^{-1}\mathbf{H})^{-1}\mathbf{H}^H\mathbf{S}^{-1}\mathbf{x}}. \tag{9}$$

It follows from (2), (4), (8), and (9) that

$$t_{\mathrm{SAMF}} = \frac{t_{\mathrm{SGLRT}}}{\beta} \tag{10}$$

and

$$t_{\mathrm{ASD}} = \frac{t_{\mathrm{SGLRT}}}{1-\beta}. \tag{11}$$

Using (10) and (11) one can rewrite (5) as

$$t_{\mathrm{SAMF\text{–}ASD}} = \left(\frac{\alpha}{\beta}+\frac{1-\alpha}{1-\beta}\right)t_{\mathrm{SGLRT}}\ . \tag{12}$$

It follows that (7) can be recast as

$$\begin{aligned}\mathrm{PD} &= \Pr\left[\left(\frac{\alpha}{\beta}+\frac{1-\alpha}{1-\beta}\right)t_{\mathrm{SGLRT}} > \eta_{\mathrm{w}};\ \mathrm{H}_1\right]\\ &= \Pr\left[t_{\mathrm{SGLRT}} > \frac{\eta_{\mathrm{w}}\beta(1-\beta)}{\alpha-2\alpha\beta+\beta};\ \mathrm{H}_1\right].\end{aligned} \tag{13}$$

Remarkably, to guarantee the PD in (13) meaningful, the following constraint is needed

$$\frac{\beta(1-\beta)}{\alpha-2\alpha\beta+\beta} > 0. \tag{14}$$

It is known from (9) that

$$0 \le \beta \le 1. \tag{15}$$

It follows that

$$\beta(1-\beta) \ge 0. \tag{16}$$

Hence, we only need to guarantee

$$\alpha-2\alpha\beta+\beta > 0, \tag{17}$$

from which

$$(1-2\alpha)\beta > -\alpha. \tag{18}$$

According to (6) and (15), we have

$$\begin{cases}\beta > 0, & \text{when } 0 \le \alpha < \dfrac{1}{2}\\ \beta < \dfrac{\alpha}{2\alpha-1}, & \text{when } \dfrac{1}{2} \le \alpha \le 1\end{cases} \tag{19}$$

Using (6) again leads to

$$\frac{\alpha}{2\alpha-1} > 1, \ \text{when } \frac{1}{2} \le \alpha \le 1. \tag{20}$$

As a result, we obtain

$$\begin{cases}\beta > 0, & \text{when } 0 \le \alpha < \dfrac{1}{2}\\ \beta < 1, & \text{when } \dfrac{1}{2} \le \alpha \le 1\end{cases} \tag{21}$$

Gathering (21) and (15), it is known that the inequality in (17) holds with probability unity under the constraints (15) and (6). As a result, (14) holds true.

The conditional PD, with given β, can be expressed as

$$\mathrm{PD}_\beta = 1-\mathcal{P}_1\left[\frac{\eta_{\mathrm{w}}\beta(1-\beta)}{\alpha-2\alpha\beta+\beta}\right], \tag{22}$$

where $\mathcal{P}_1(\eta)$ is the cumulative distribution function (CDF) of t_{SGLRT} with β fixed under hypothesis H_1, defined as

$$\mathcal{P}_1(\eta) = \Pr[t_{\mathrm{SGLRT}} \le \eta;\ \mathrm{H}_1], \tag{23}$$

where η is positive real number.

It is known from [36] that the SGLRT in (8), for given β, is distributed as a complex noncentral F-distribution with p and $L-N+1$ degrees of freedom (DOFs) and a noncentrality parameter ρ_ϕ, denoted symbolically as

$$t_{\mathrm{SGLRT}\,|\beta;\mathrm{H}_1} \sim \mathcal{CF}_{p,L-N+1}(\beta\rho_\phi), \tag{24}$$

where

$$\rho_\phi = \rho\cos^2\phi, \tag{25}$$

$$\rho = \mathbf{s}_0^H\mathbf{R}^{-1}\mathbf{s}_0 \tag{26}$$

is the signal-to-noise ratio (SNR), and

$$\cos^2\phi = \frac{\mathbf{s}_0^H\mathbf{R}^{-1}\mathbf{H}(\mathbf{H}^H\mathbf{R}^{-1}\mathbf{H})^{-1}\mathbf{H}^H\mathbf{R}^{-1}\mathbf{s}_0}{\mathbf{s}_0^H\mathbf{R}^{-1}\mathbf{s}_0} \tag{27}$$

is the cosine squared between the whitened actual signal $\mathbf{s}_0$ and whitened nominal signal subspace spanned by the columns of $\mathbf{H}$.

According to the equation (A2-29) in [39],

$$\mathcal{P}_1(\eta) = \sum_{k=0}^{L-N} \mathrm{C}_{L-N+p}^{k+p}\frac{\eta^{k+p}}{(1+\eta)^{L-N+p}}\ \mathrm{IG}_{k+1}\left[\frac{\rho_\phi\beta}{1+\eta}\right], \tag{28}$$

where

$$\mathrm{C}_n^m = \frac{n!}{m!(n-m)!} \tag{29}$$

is the binominal coefficient and

$$\mathrm{IG}_{k+1}(a) = e^{-a}\sum_{m=0}^{k}\frac{a^m}{m!} \tag{30}$$

is the incomplete Gamma function.

Substituting (28) into (22) results in the conditional PD of the SAMF-ASD. Averaging the conditional PD given in (22) over β in the range from 0 to 1 yields the unconditional PD, described as

$$\mathrm{PD} = 1-\int_0^1 \mathcal{P}_1\left[\frac{\eta_{\mathrm{w}}\beta(1-\beta)}{\alpha-2\alpha\beta+\beta}\right]f_1(\beta)\ \mathrm{d}\beta, \tag{31}$$

where $f_1(\beta)$ is the probability density function (PDF) of the loss factor β in (9) under hypothesis H_1. The loss factor β in (9) under hypothesis H_1 in the presence of subspace signal mismatch is distributed as a complex noncentral Beta-distribution with $L-N+p+1$ and $N-p$ DOFs and a noncentrality parameter δ^2, written symbolically as

$$\beta_{\mathrm{H}_1} \sim \mathcal{CB}_{L-N+p+1,N-p}(\delta^2), \tag{32}$$

where

$$\delta^2 = \rho\ \sin^2\phi, \tag{33}$$

$\sin^2\phi = 1-\cos^2\phi$, and $\cos^2\phi$ is given in (27).

Moreover, according to (32) and using (A2-23) in [39], one obtains

$$f_1(\beta) = \mathrm{e}^{\delta^2\beta}\sum_{k=0}^{L-N+p+1}\mathrm{C}_{L-N+p+1}^{k}\frac{L!}{(L+k)!}\delta^{2k}f_0(\beta), \tag{34}$$

where $f_0(\beta)$ is the PDF of β under H_0, given by

$$f_0(\beta) = \frac{\beta^{L-N+p}(1-\beta)^{N-p-1}}{\mathrm{B}(L-N+p+1,N-p)}, \tag{35}$$

with

$$\mathrm{B}(m,n) = \frac{(m-1)!(n-1)!}{(m+n-1)!} \tag{36}$$

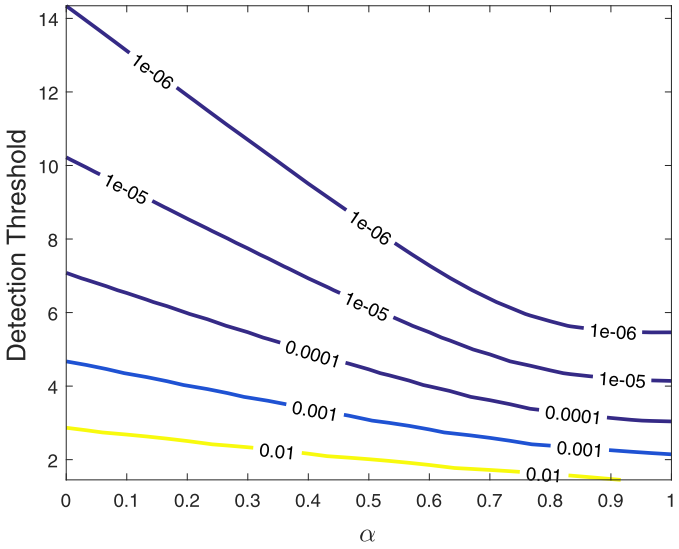

Fig. 1. Contour of the PFA of the SAMF-ASD versus the detection threshold and weight α.

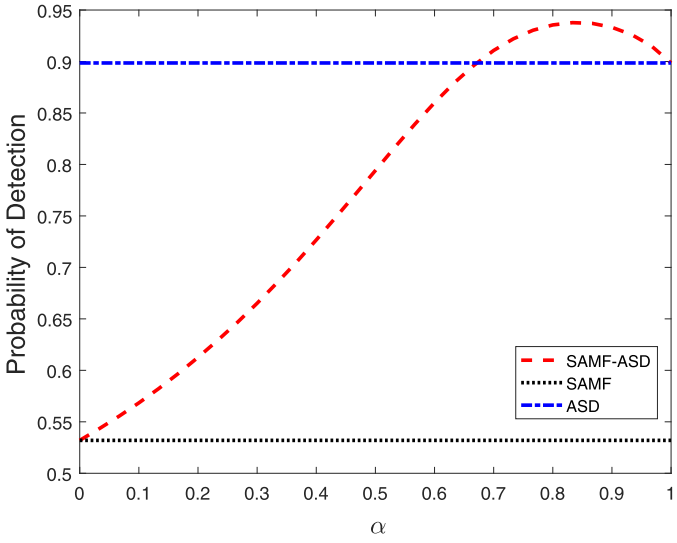

Fig. 2. PD of the SAMF-ASD versus the weight α in the absence of signal mismatch.

being the Beta function with integer argument. Hence, substituting (28) and (34) into (31) results in the final PD.

Under hypothesis H_0, no signal exists. Hence, (24) and (32) degenerate into

$$t_{\mathrm{SGLRT}\,|\mathrm{H}_0} \sim \mathcal{CF}_{p,L-N+1} \tag{37}$$

and

$$\beta_{\mathrm{H}_0} \sim \mathcal{CB}_{L-N+p+1,N-p}, \tag{38}$$

respectively. In a manner similar to (31), the PFA is given by

$$\mathrm{PFA} = 1 - \int_0^1 \mathcal{P}_0\left[\frac{\eta_{\mathrm{w}}\beta(1-\beta)}{\alpha - 2\alpha\beta + \beta}\right] f_0(\beta)\, \mathrm{d}\beta, \tag{39}$$

where $\mathcal{P}_0(\eta)$ is the CDF of t_{SGLRT} under hypothesis H_0, namely,

$$\mathcal{P}_0(\eta) = \Pr[t_{\mathrm{SGLRT}} \le \eta;\ \mathrm{H}_0]. \tag{40}$$

Equation (28), with ρ replaced by zero, becomes

$$\mathcal{P}_0(\eta) = \sum_{k=0}^{L-N} \mathrm{C}_{L-N+p}^{k+p} \frac{\eta^{k+p}}{(1+\eta)^{L-N+p}}. \tag{41}$$

Substituting (35) and (41) into (39) results in the final PFA.

4. Numerical examples

Numerical examples are given in this section to demonstrate the detection performance of the proposed SAMF-ASD. For independent verification of the derived expressions for the PD and PFA, Monte Carlo simulations are provided, besides the theoretical results. For the MC simulations, 10^4 and 10^8 independent trials are run to evaluate the PD and detection threshold, respectively. The detection threshold is needed to ensure a preassigned PFA. The (i, j)th component of $\mathbf{R}$ is chosen to be $\sigma_n^2 \varepsilon^{|i-j|}$, $i, j = 1, 2, \cdots, N$, where σ_n^2 denotes the noise power and ε is the one-lag correlation coefficient. The following parameters are used throughout the paper: $N = 12$, $p = 3$, $L = 2N$, $\sigma_n^2 = 1$, and $\varepsilon = 0.95$. Moreover, the PFA is set to be 10^{-6} in all figures except for Fig. 1.

Fig. 1 shows the contours of the SAMF-ASD under different weights and detection thresholds. It is seen that for a given PFA, one has freedom to choose a suitable weight α. The best choice for the weight in the case of no signal mismatch is the one that achieves the largest PD. On the other hand, when subspace signal mismatch happens, one can choose a weight that provides robustness or selectivity, depending on system requirements. In addition, it is shown in Fig. 1 that the PFA decreases as the weight and/or the detection threshold increase.

Fig. 2 displays the PD of the SAMF-ASD with different weights in the absence of signal mismatch. The SNR is set to be 20 dB. The results highlight that the PD of the SAMF-ASD first increases and then decreases with the increase of the weight. The SAMF-ASD has the same detection performance as the ASD and SAMF at $\alpha = 0$ and $\alpha = 1$, respectively. This is because the SAMF-ASD reduces to the ASD and SAMF at the corresponding values of α. A remarkable feature is that the SAMF-ASD achieves slightly better detection performance than the SAMF and ASD in the range of $0.7 < \alpha < 1$ in this example. The best α in the absence of signal mismatch is the one with which the weighted detector SAMF-ASD provides the highest PD. Unfortunately, an explicit expression for the best α is unavailable. Alternatively, we can use the closed-form expression for the PD given in (31) to numerically search the best α which achieves the highest PD.

Fig. 3 plots the PD of the SAMF-ASD under different SNRs in the case of no signal mismatch. The weight α is chosen as 0.83 for the SAMF-ASD. For comparison purposes, the PDs of the SAMF and ASD are also shown. For the SAMF-ASD, the dashed line denotes the theoretical result, while the symbol circle stands for MC result. The results highlight that the theoretical PD of the SAMF-ASD is in good agreement with the MC simulation, and the proposed weighted detector with $\alpha = 0.83$ outperforms the SAMF and ASD.

Fig. 4 demonstrates the detection performance of the SAMF-ASD with the weight as a parameter when subspace signal mismatch arises. The SNR is set to be 24 dB. For the curves of the SAMF-ASD, the dashed line, dotted line, and dash-dotted line stand for the theoretical results, while the symbols square, circle, and triangle denote MC results. It is indicated that the theoretical results comply with the MC results pretty well. For comparison, the PDs of the SAMF and ASD are also given. It can be observed that the SAMF-ASD is much more flexible in governing the detection performance for mismatched subspace signals. When the weight α is large, the SAMF-ASD is very robust to mismatched subspace signals. In contrast, when α is small, the SAMF-ASD is very selective to mismatched subspace signals.

Fig. 5 presents the contours of the PD of the SAMF-ASD, as a function of $\cos^2\phi$ and SNR. This type of figure is a generalization of Fig. 4. The results in Fig. 5 clearly show that the SAMF-

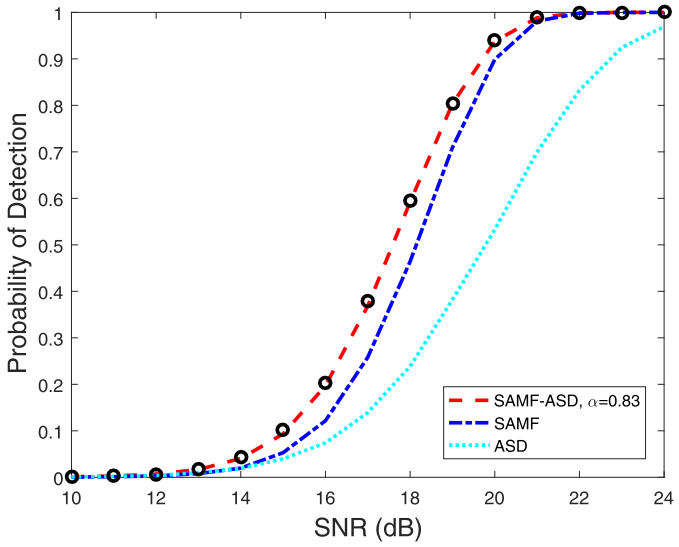

Fig. 3. PDs of the detectors under different SNRs in the absence of signal mismatch. For the SAMF-ASD, the dashed line denotes the theoretical result, while the symbol circle (○) stands for MC results.

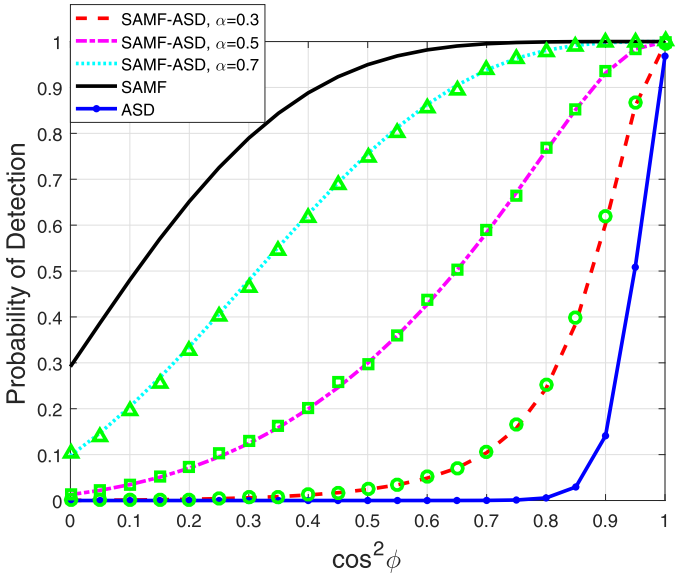

Fig. 4. PDs of the detectors under different $\cos^2\phi$ in the presence of subspace signal mismatch. For the SAMF-ASD the dashed line, dotted line, and dash-dotted line denote the theoretical results, while the symbols square (□), circle (○), and triangle (△) stand for MC results.

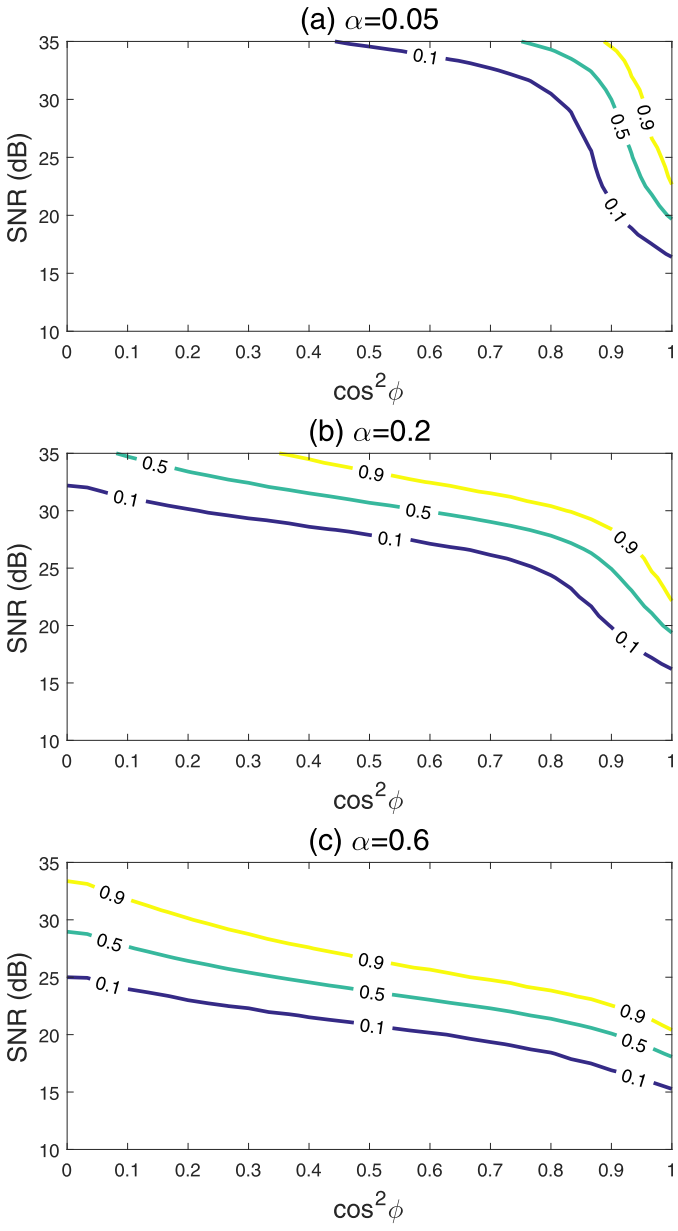

Fig. 5. Contour of PD of the SAMF-ASD in the presence of subspace signal mismatch.

ASD can flexibly control the detection performance for mismatched subspace signals. With a moderately large weight α, the SAMF-ASD is very robust. For example, when the amount of signal mismatch is large as $\cos^2\phi < 0.5$, the SAMF-ASD with $\alpha = 0.6$ can provide a PD of 0.9 when the SNR is larger than 26.5 dB. In contrast, with a small α, the SAMF-ASD becomes very selective. Only when the amount of signal mismatch is small as $\cos^2\phi > 0.9$, it achieves a PD of 0.9.

5. Conclusions

In this paper, a weighted detector for mismatched subspace signal detection, was proposed, namely, the SAMF-ASD. It is constructed by linearly combining the SAMF and ASD. Analytical expressions for the PD and PFA are derived. The SAMF-ASD can control its robustness or selectivity in the presence of subspace signal mismatch by adjusting the weight. Specifically, a relative large value of the weight is needed, when a robust detector is needed, such as operating the radar system in surveillance model. Moreover, a small value of the weight is needed, when a selective detector is needed, such as operating the radar system in tracking model.

Acknowledgments

This work was supported in part by National Natural Science Foundation of China under Contracts 61501351 and 61501505.

References

[1] E.J. Kelly, An adaptive detection algorithm, IEEE Trans. Aerosp. Electron.Syst. 22 (1) (1986) 115–127.
[2] W.-S. Chen, I.S. Reed, A new CFAR detection test for radar, Digital Signal Process. 1 (4) (1991) 198–214.
[3] F.C. Robey, D.R. Fuhrmann, E.J. Kelly, R. Nitzberg, A CFAR adaptive matched filter detector, IEEE Trans. Aerosp. Electron.Syst. 28 (1) (1992) 208–216.

[4] A. De Maio, Rao test for adaptive detection in Gaussian interference with unknown covariance matrix, IEEE Trans. Signal Process. 55 (7) (2007) 3577–3584.
[5] S. Kraut, L.L. Scharf, The CFAR adaptive subspace detector is a scale-invariant GLRT, IEEE Trans. Signal Process. 47 (9) (1999) 2538–2541.
[6] G. Cui, L. Kong, X. Yang, Multiple-input multiple-output radar detectors design in non-Gaussian clutter, IET Radar Sonar Navig. 4 (5) (2010) 724–732.
[7] J. Guan, X. Zhang, Subspace detection for range and Doppler distributed targets with Rao and Wald tests, Signal Process. 91 (1) (2011) 51–60.
[8] G. Cui, L. Kong, X. Yang, GLRT-based detection algorithm for polarimetric MIMO radar against SIRV clutter, Circuits Syst. Signal Process. 31 (3) (2012) 1033–1048.
[9] A. Aubry, A. De Maio, L. Pallotta, A. Farina, Radar detection of distributed targets in homogeneous interference whose inverse covariance structure is defined via unitary invariant functions, IEEE Trans. Signal Process. 61 (20) (2013) 4949–4961.
[10] J. Liu, Z.-J. Zhang, Y. Cao, M. Wang, Distributed target detection in subspace interference plus Gaussian noise, Signal Process. 85 (2014) 88–100.
[11] G. Cui, J. Liu, H. Li, B. Himed, Signal detection with noisy reference for passive sensing, Signal Process. 108 (2015) 389–399.
[12] S. Lei, Z. Zhao, Z. Nie, Q.-H. Liu, Adaptive polarimetric detection method for target in partially homogeneous background, Signal Process. 106 (2015) 301–311.
[13] Z. Wang, M. Li, H. Chen, Y. Lu, R. Cao, P. Zhang, L. Zuo, Y. Wu, Persymmetric detectors of distributed targets in partially homogeneous disturbance, Signal Process. 128 (2016) 382–388.
[14] A. De Maio, D. Orlando, C. Hao, G. Foglia, Adaptive detection of point-like targets in spectrally symmetric interference, IEEE Trans. Signal Process. 64 (12) (2016) 3207–3220.
[15] C. Hao, D. Orlando, G. Foglia, G. Giunta, Knowledge-based adaptive detection: joint exploitation of clutter and system symmetry properties, IEEE Signal Process. Lett. 23 (10) (2016) 1489–1493.
[16] A. Hariri, M. Babaie-Zadeh, Compressive detection of sparse signals in additive white Gaussian noise without signal reconstruction, Signal Process. 131 (2017) 376–385.
[17] N.B. Pulsone, C.M. Rader, Adaptive beamformer orthogonal rejection test, IEEE Trans. Signal Process. 49 (3) (2001) 521–529.
[18] D. Orlando, G. Ricci, A Rao test with enhanced selectivity properties in homogeneous scenarios, IEEE Trans. Signal Process. 58 (10) (2010) 5385–5390.
[19] A. De Maio, D. Orlando, A survey on two-stage decision schemes for point-like targets in Gaussian interference, IEEE Aerosp. Electron. Syst. Mag. 31 (4) (2016) 20–29.
[20] C.D. Richmond, Performance of the adaptive sidelobe blanker detection algorithm in homogeneous environments, IEEE Trans. Signal Process. 48 (5) (2000) 1235–1247.
[21] N.B. Pulsone, M.A. Zatman, A computationally efficient two-step implementation of the GLRT, IEEE Trans. Signal Process. 48 (3) (2000) 609–616.
[22] F. Bandiera, O. Besson, D. Orlando, G. Ricci, An improved adaptive sidelobe blanker, IEEE Trans. Signal Process. 56 (9) (2008a) 4152–4161.
[23] F. Bandiera, D. Orlando, G. Ricci, A subspace-based adaptive sidelobe blanker, IEEE Trans. Signal Process. 56 (9) (2008b) 4141–4151.
[24] F. Bandiera, D. Orlando, G. Ricci, One- and two-stage tunable receivers*, IEEE Trans. Signal Process. 57 (8) (2009) 3264–3273.
[25] C. Hao, B. Liu, L. Cai, Performance analysis of a two-stage Rao detector, Signal Process. 91 (8) (2011) 2141–2146.
[26] S.Z. Kalson, An adaptive array detector with mismatched signal rejection, IEEE Trans. Aerosp. Electron.Syst. 28 (1) (1992) 195–207.
[27] C. Hao, B. Liu, S. Yan, L. Cai, Parametric adaptive radar detector with enhanced mismatched signals rejection capabilities, EURASIP J. Adv. Signal Process. 2010 (2010).
[28] W. Liu, W. Xie, Y. Wang, Parametric detector in the situation of mismatched signals, IET Radar Sonar Navig. 8 (1) (2014) 48–53.
[29] J. Liu, Z.-J. Zhang, Y. Yang, Performance enhancement of subspace detection with a diversely polarized antenna, IEEE Signal Process. Lett. 19 (1) (2012) 4–7.
[30] A. Zeira, B. Friedlander, Robust subspace detectors, in: The 31th Asilomar Conference on Signals, Systems and Computers, 1, 1997, pp. 778–782.
[31] A. Zeira, B. Friedlander, Robust adaptive subspace detectors for space time processing, in: IEEE International Conference on Acoustics, Speech and Signal Processing (ICASSP), 4, 1998, pp. 1965–1968.
[32] O. Besson, L.L. Scharf, S. Kraut, Adaptive detection of a signal known only to lie on a line in a known subspace, when primary and secondary data are partially homogeneous, IEEE Trans. Signal Process. 54 (12) (2006) 4698–4705.
[33] J. Liu, Z.-J. Zhang, Y. Yang, Optimal waveform design for generalized likelihood ratio and adaptive matched filter detectors using a diversely polarized antenna, Signal Process. 92 (4) (2012) 1126–1131.
[34] S. Kraut, L.L. Scharf, Adaptive subspace detectors, IEEE Trans. Signal Process. 49 (1) (2001) 1–16.
[35] W. Liu, W. Xie, J. Liu, Y. Wang, Adaptive double subspace signal detection in Gaussian backgroundpart I: homogeneous environments, IEEE Trans. Signal Process. 62 (9) (2014) 2345–2357.
[36] W. Liu, J. Liu, C. Zhang, H. Li, Performance prediction of subspace-based adaptive detectors with signal mismatch, Signal Process. 123 (2016) 122–126.
[37] S. Bose, A.O. Steinhardt, Adaptive array detection of uncertain rank one waveforms, IEEE Trans. Signal Process. 44 (11) (1996) 2801–2809.
[38] D. Pastina, P. Lombardo, T. Bucciarelli, Adaptive polarimetric target detection with coherent radar part I: detection against Gaussian background, IEEE Trans. Aerosp. Electron.Syst. 37 (4) (2001) 1194–1206.
[39] E.J. Kelly, K.M. Forsythe, Adaptive detection and parameter estimation for multidimensional signal models, Technical Report, Lincoln Laboratory, Lexington, 1989.